

# Prior starvation mitigates acute doxorubicin cardiotoxicity through restoration of autophagy in affected cardiomyocytes

Tomonori Kawaguchi<sup>1</sup>, Genzou Takemura<sup>1\*</sup>, Hiromitsu Kanamori<sup>1</sup>, Toshiaki Takeyama<sup>1</sup>, Takatomo Watanabe<sup>1</sup>, Kentaro Morishita<sup>1</sup>, Atsushi Ogino<sup>1</sup>, Akiko Tsujimoto<sup>1</sup>, Kazuko Goto<sup>1</sup>, Rumi Maruyama<sup>1</sup>, Masanori Kawasaki<sup>1</sup>, Atsushi Mikami<sup>1</sup>, Takako Fujiwara<sup>2</sup>, Hisayoshi Fujiwara<sup>3</sup>, and Shinya Minatoguchi<sup>1</sup>

<sup>1</sup>Department of Cardiology, Gifu University Graduate School of Medicine, 1-1 Yanagido, Gifu 501-1194, Japan; <sup>2</sup>Department of Food Science, Kyoto Women's University, Kyoto, Japan; and <sup>3</sup>Department of Cardiology, Hyogo Prefectural Amagasaki Hospital, Amagasaki, Japan

Received 3 January 2012; revised 9 August 2012; accepted 3 September 2012; online publish-ahead-of-print 5 September 2012

Time for primary review: 39 days

<b>Aims</b>	Active autophagy has recently been reported in doxorubicin-induced cardiotoxicity; here we investigated its pathophysiological role.
<b>Methods and results</b>	Acute cardiotoxicity was induced in green fluorescent protein-microtubule-associated protein 1 light chain 3 (GFP-LC3) transgenic mice by administering two intraperitoneal injections of 10 mg/kg doxorubicin with a 3 day interval. A starvation group was deprived of food for 48 h before each injection to induce autophagy in advance. Doxorubicin treatment caused left ventricular dilatation and dysfunction within 6 days. Cardiomyocyte autophagy appeared to be activated in the doxorubicin group, based on LC3, p62, and cathepsin D expression, while it seemed somewhat diminished by starvation prior to doxorubicin treatment. Unexpectedly, however, myocardial ATP levels were reduced in the doxorubicin group, and this reduction was prevented by earlier starvation. Electron microscopy revealed that the autophagic process was indeed initiated in the doxorubicin group, as shown by the increased lysosomes, but was not completed, i.e. autophagolysosome formation was rare. Starvation prior to doxorubicin treatment partly restored autophagosome formation towards control levels. Autophagic flux assays in both <i>in vivo</i> and <i>in vitro</i> models confirmed that doxorubicin impairs completion of the autophagic process in cardiomyocytes. The activities of both AMP-activated protein kinase and the autophagy-initiating kinase unc-51-like kinase 1 (ULK1) were found to be decreased by doxorubicin, and these were restored by prior starvation.
<b>Conclusion</b>	Prior starvation mitigates acute doxorubicin cardiotoxicity; the underlying mechanism may be, at least in part, restoration and further augmentation of myocardial autophagy, which is impaired by doxorubicin, probably through inactivation of AMP-activated protein kinase and ULK1.
<b>Keywords</b>	Autophagy • Doxorubicin • Heart failure

## 1. Introduction

Autophagy is a highly regulated, dynamic process involving degradation of cytosolic proteins and organelles through engulfment into double-membraned vesicles called autophagosomes, which in turn fuse with lysosomes for digestion of the contents. More than 30 ATG (autophagy-related) genes required for autophagy and its

related pathways have been identified and these are now classified into the following six functional groups: (i) the Atg1 kinase complex (Atg1-13-17-29-31); (ii) Atg9; (iii) the class III phosphatidylinositol (PI)3-kinase complex (Atg6-Atg14-Vps15-Vps34); (iv) the PI(3)P-binding Atg2-Atg18 complex; (v) the Atg12 conjugation system (Atg12-Atg5-Atg16); and (vi) the Atg8 conjugation system (Atg8-PE).<sup>1,2</sup> The mammalian homologue of Atg8, microtubule-associated protein 1 light

\* Corresponding author. Tel: +81 58 230 6542; Fax: +81 58 230 6524, E-mail: gt@gifu-u.ac.jp

chain 3 (LC3), is converted from LC3-I into the phosphatidylethanolamine (PE)-conjugated form LC3-II, and this is the only protein marker that is reliably associated with completed autophagosomes. During autophagic digestion, degraded membrane lipids and proteins within autophagosomes are recruited to maintain needed levels of ATP production and protein synthesis, thereby promoting cell survival.<sup>3</sup> Autophagy also plays important roles in cell growth and development, organelle biogenesis and turnover, and in controlling the balance between protein synthesis and degradation.<sup>4–6</sup> Autophagy occurs constitutively in the healthy heart, and its activity is substantially increased in cases of failing hearts, hypertrophied hearts, and ischaemic hearts.<sup>7–10</sup> Inefficient autophagy causes the myocardium to function poorly, and pharmacological inhibition of starvation-induced autophagy results in heart failure.<sup>11</sup> Autophagy has also been shown to be an adaptive response of the heart, protecting the myocardium from haemodynamic overload and acute ischaemic death.<sup>12–14</sup> On the contrary, autophagy is a mode of cell death that primarily occurs during tissue and organ development to eliminate unnecessary cells in normal circumstances.<sup>15</sup> Consistent with its dual nature, however, studies suggest that autophagy acts as a double-edged sword when the heart is under stress; while it functions to remove protein aggregates and damaged organelles as a means of maintaining energy homeostasis, its enhancement can also lead to cell death.<sup>8,16–21</sup> At present, the functional role of autophagy in heart disease (i.e. whether it mediates cell survival or cell death) and whether it up- or down-regulates cellular function is still poorly understood.

The anti-neoplastic drug doxorubicin (DOX; adriamycin) is effective in the treatment of a broad range of haematogenous and solid human malignancies, but its clinical use is limited by its dose-dependent side-effects, namely irreversible degenerative cardiomyopathy and congestive heart failure.<sup>22–24</sup> It is widely thought that free radical-induced mitochondrial damage contributes to DOX-induced cardiotoxicity.<sup>25</sup> In addition, DOX can induce DNA damage, inhibit DNA and protein synthesis, promote myofibril degeneration, inhibit transcription of specific gene programmes, and induce cardiomyocyte apoptosis via a caspase-3-dependent mechanism. One recent study reported that DOX treatment induces acute cardiac dysfunction and reduces cardiac mass via p53-dependent inhibition of mammalian target of rapamycin (mTOR) signalling, and that it is the loss of myocardial mass, not cardiomyocyte apoptosis, that is the major contributor to acute DOX cardiotoxicity.<sup>26</sup> However, because DOX can interfere with many different intracellular processes, it has proved difficult to determine the molecular aetiologies of its acute and chronic cardiotoxicity precisely. Notably in that regard, another recent study has suggested that autophagic cardiomyocyte death contributes to the pathogenesis of DOX-induced cardiomyopathy.<sup>27</sup> However, the true role of autophagy in DOX cardiotoxicity is still unclear because there has been little documentation of autophagic cardiomyocytes in the DOX-treated heart. In the present study, therefore, we examined autophagy and tried to determine its pathophysiological significance in the mouse heart with acute DOX cardiotoxicity.

## 2. Methods

### 2.1 Animals and experimental protocols

This study conforms to the *Guide for the Care and Use of Laboratory Animals* published by the US National Institutes of Health (NIH publication no. 85-23, revised 1996) and was approved by our Institutional Animal

Research Committee. Pathogen-free heterozygous green fluorescent protein-labelled microtubule-associated protein 1 light chain 3 (GFP-LC3) transgenic mice (strain GFP-LC3#53; RIKEN BioResource Center, Tsukuba, Japan) harbouring a rat LC3-enhanced GFP fusion construct under the control of the chicken  $\beta$ -actin promoter,<sup>28</sup> were housed in a temperature-controlled environment with 12 h–12 h light–dark cycles and received food and water *ad libitum*. Genotyping of GFP-LC3 offspring was carried out by PCR analysis as previously reported.<sup>11,28</sup>

Adult mice received DOX (two intraperitoneal injections of 10 mg/kg at 3 day intervals; 20 mg/kg cumulative dose) or vehicle (saline), and were killed 5 days after the initial injection (see Supplementary material online, *Figure S1A*). Although the mice were usually fed *ad libitum*, some were deprived of food for 2 days before each injection of saline or DOX. Water was provided *ad libitum* to all groups.

### 2.2 Physiological studies

Echocardiography and cardiac catheterization were carried out before the mice were killed, as described previously.<sup>11</sup> Animals were anaesthetized with an intraperitoneal injection of pentobarbital (30 mg/kg) for each examination. The adequacy of anaesthesia was assessed by monitoring ECG and respiratory rate. This relatively small dose of pentobarbital did not affect the level of blood pressure, the heart rate, or the state of respiration in mice with any treatment. Echocardiograms were recorded using an echocardiographic system (Vevo770; Visualsonics, Toronto, Canada) equipped with a 45 MHz imaging transducer. Following echocardiography, the right carotid artery was cannulated with a micromanometer-tipped catheter (SPR 671; Millar Instrument, Houston, TX, USA) that was advanced into the aorta and then into the left ventricle to record the pressure and maximal and minimal maximal and minimal first derivative of left ventricular pressure ( $\pm$  dP/dt).

### 2.3 Histology

Once the physiological measurements were complete, all mice were killed with an overdose pentobarbital (50 mg/kg i.p.). Then the hearts were removed, weighed, and cut into two transverse slices through the middle of the ventricles between the atrioventricular groove and the apex. The basal specimens were fixed in 10% buffered formalin, embedded in paraffin, cut into 4- $\mu$ m-thick sections, and stained with haematoxylin and eosin, Masson's trichrome, or sirius red F3BA (Aldrich, St. Louis, MO, USA). Quantitative assessments, including cardiomyocyte size (expressed as the transverse diameter of the myocyte cut at the level of the nucleus), cell number, and the area of fibrosis, were carried out in 20 randomly chosen high-power fields ( $\times$ 400) in each section using a multipurpose colour image processor (LUZEX F; Nireco, Kyoto, Japan).

### 2.4 Immunohistochemistry

After deparaffinization, the 4- $\mu$ m-thick sections were incubated with a primary anti-GFP antibody (Molecular Probes, Eugene, OR, USA). A Vectastain Elite ABC system (Vector Laboratories, Burlingame, CA, USA) was then used to immunostain the sections; diaminobenzidine served as the chromogen, and the nuclei were counterstained with haematoxylin. Alternatively, the anti-GFP primary antibody was labelled with an Alexa 488-conjugated secondary antibody (Molecular Probes), and rhodamine-phalloidine (Invitrogen, Carlsbad, CA, USA) was overlaid on the labelled sections to identify the cardiomyocytes. The sections were then counterstained with Hoechst 33342 and observed under a confocal microscope (LSM510; Zeiss, Oberkochen, Germany).

Sections were also subjected to *in situ* terminal dUTP nick end-labelling (TUNEL) using an ApopTag kit (Chemicon, Temecula, CA, USA) according to the manufacturer's instructions. In order to evaluate apoptosis separately among cardiomyocytes and non-cardiomyocytes in the heart, the sections were double labelled using TUNEL (Fluorescein-FragEL; Oncogene, Cambridge, MA, USA) and rhodamine-phalloidine. Nuclei were

stained with Hoechst 33342. Mouse mammary tissue served as a positive control for the TUNEL assay.

## 2.5 Electron microscopy

Cardiac tissue was quickly cut into 1 mm cubes, immersion fixed in 2.5% glutaraldehyde in 0.1 mol/L phosphate buffer (pH 7.4) overnight at 4°C, and postfixed in 1% buffered osmium tetroxide. The specimens were then dehydrated through a graded ethanol series and embedded in epoxy resin. Ultrathin sections (90 nm) double stained with uranyl acetate and lead citrate were then examined under an electron microscope (H-800; Hitachi, Tokyo, Japan).

## 2.6 Western blotting

Proteins (50 µg) extracted from hearts ( $n = 4-6$  from each group) were subjected to 10 or 15% PAGE and then transferred onto polyvinylidene difluoride membranes. The membranes were then probed using primary antibodies against LC3, p62 (both from MBL, Nagoya, Japan), AMP-activated protein kinase (AMPK), phosphorylated AMPK (p-AMPK; both from Cell Signaling, Beverly, MA, USA), unc-51-like kinase 1 (ULK1) (no. 10900; Santa Cruz, Santa Cruz, CA, USA) and phosphorylated ULK1 (p-ULK1; no. 6888; Cell Signaling), after which the blots were visualized using enhanced chemiluminescence (ECL; Amersham, Buckinghamshire, UK).  $\alpha$ -Tubulin (analysed using an antibody from Santa Cruz) served as the loading control.

## 2.7 ATP measurement

Myocardial ATP content was measured using an ATP bioluminescent assay kit (TOYO Ink, Tokyo, Japan) according to the manufacturer's instructions. Experiments were performed in triplicate for each group.

## 2.8 Autophagic flux assay

We investigated autophagic flux *in vivo* using the previously described method.<sup>29,30</sup> Mice received DOX (an intraperitoneal injection of 10 mg/kg) or saline, and were killed 2 days after the injection (see Supplementary material online, *Figure S1B*). Four hours before the animals were killed, chloroquine (10 mg/kg; Sigma) was injected intraperitoneally to inhibit lysosome activity. After death, the hearts were immediately harvested, and the apical half was fixed in 10% formalin for preparation of paraffin-embedded sections and examined for cardiac autophagy under a confocal microscope. The basal half was used for western blotting.

## 2.9 Cell culture and treatments

Cardiomyocytes were isolated from 1-day-old neonatal GFP-LC3#53 mice by the previously reported method.<sup>31</sup> The cardiomyocytes were plated on laminin-coated slide glass chambers and incubated in Dulbecco's Modified Eagle Medium (D-MEM) (Sigma) containing 10% fetal bovine serum (Sigma) at 37°C (see Supplementary material online, *Figure S2A*). Two days after plating, the culture medium of some chambers was replaced with glucose-free D-MEM (no. 0983; GIBCO, Carlsbad, CA, USA), in which glucose was replaced with 11 mmol/L mannitol to induce starvation-induced autophagy, and the cells were incubated for another 2 days. The cells were then treated with DOX dissolved in the D-MEM containing glucose and fetal bovine serum at the concentration of 0.1 DOX µmol/L or with saline of the same volume for 6 h. Two days later, the cells were used for immunohistochemistry for LC3-GFP, with anti-GFP antibody as the primary antibody and DAB as the chromogen, under a Vectastain Elite ABC system.

For *in vitro* autophagic flux assay, some chambers were supplemented with chloroquine at a concentration of 3 µmol/L 4 h prior to fixation after incubation in the DOX-containing medium for 6 h (see Supplementary material online, *Figure S2B*).<sup>29</sup> They were used for immunohistochemistry for LC3-GFP as described above.

## 2.10 Statistical analysis

Data are expressed as the means  $\pm$  SEM. The significance of differences between groups was evaluated using one-way ANOVA with a *post hoc* Newman-Keul's multiple comparisons test. Values of  $P < 0.05$  were considered significant.

## 3. Results

### 3.1 Cardiac function

Five days after the initial administration of DOX, all of the mice in each group remained alive. The results of our physiological studies are summarized in *Figure 1*. Echocardiography and cardiac catheterization showed that 5 days after the initial administration of DOX or saline, mice receiving DOX without prior starvation had significant cardiac deterioration characterized by enlargement of the left ventricular (LV) cavity (LVDD;  $3.9 \pm 0.25$  mm) and signs of reduced cardiac function, i.e. increased LV end-diastolic pressure (LVEDP;  $3.7 \pm 0.33$  mmHg) and decreased LV ejection fraction (EF;  $47 \pm 4.4\%$ ) and  $\pm$  dP/dt ( $4952 \pm 124$  and  $-2869 \pm 181$  mmHg/s) compared with the saline group (LVDD,  $3.4 \pm 0.10$  mm; LVEDP,  $0.78 \pm 0.38$  mmHg; EF,  $66 \pm 3.6\%$ ; and  $\pm$  dP/dt,  $11692 \pm 795$  and  $-8884 \pm 1279$  mmHg/s). Starvation prior to DOX administration significantly mitigated the DOX-induced impairment of cardiac function (LVDD,  $3.4 \pm 0.31$  mm; LVEDP,  $1.1 \pm 0.50$  mmHg; EF,  $64 \pm 6.5\%$ ; and  $\pm$  dP/dt,  $9409 \pm 551$  and  $-4056 \pm 230$  mmHg/s). Starvation had no effect on cardiac function in the saline group.

### 3.2 Cardiac pathology

Consistent with the echocardiography, transverse sections of hearts from DOX-treated mice showed LV dilatation, which was attenuated by prior starvation (*Figure 2A*). In addition, the heart weight-to-body weight ratios were significantly greater in DOX-treated than saline-treated mice, and this effect too was attenuated by prior starvation (saline,  $3.45 \pm 0.27$  mg/g; saline with starvation,  $3.21 \pm 0.20$  mg/g; DOX,  $3.90 \pm 0.14$  mg/g; DOX with starvation,  $3.31 \pm 0.27$  mg/g; *Figure 2B*). Despite the apparent increase in heart weight, the transverse diameters of the cardiomyocytes from DOX-treated hearts were significantly smaller than those from saline-treated hearts ( $14.79 \pm 0.46$  vs.  $13.35 \pm 0.51$  µm), and prior starvation exerted a significant protective effect against this DOX-induced atrophy (transverse diameter,  $14.17 \pm 0.57$  µm; *Figure 2A and B*). When we then assessed cardiac fibrosis using sirius red-stained sections, we found that the amount of fibrosis was significantly greater in the DOX group than the saline group ( $1.23 \pm 0.02$  vs.  $1.03 \pm 0.14\%$ ), and that the DOX-induced fibrosis was significantly reduced by prior starvation ( $1.06 \pm 0.09\%$ ; *Figure 2A and B*). TUNEL-positive cells were observed among both cardiomyocytes and non-cardiomyocytes in all four groups, but we found no significant difference in the incidence of TUNEL positivity between mice that received DOX and those that did not, and prior starvation had no significant effect on the incidence of TUNEL positivity in the heart (*Figure 2B*). Although electron microscopy revealed degenerative changes in cardiomyocytes from DOX-treated hearts, no typically apoptotic cells were found.

### 3.3 Cardiac autophagy

Our immunohistochemical analysis revealed that the numbers of LC3-GFP puncta, which develop in parallel with LC3-II expression,<sup>28</sup> increased significantly within cardiomyocytes in mice treated with

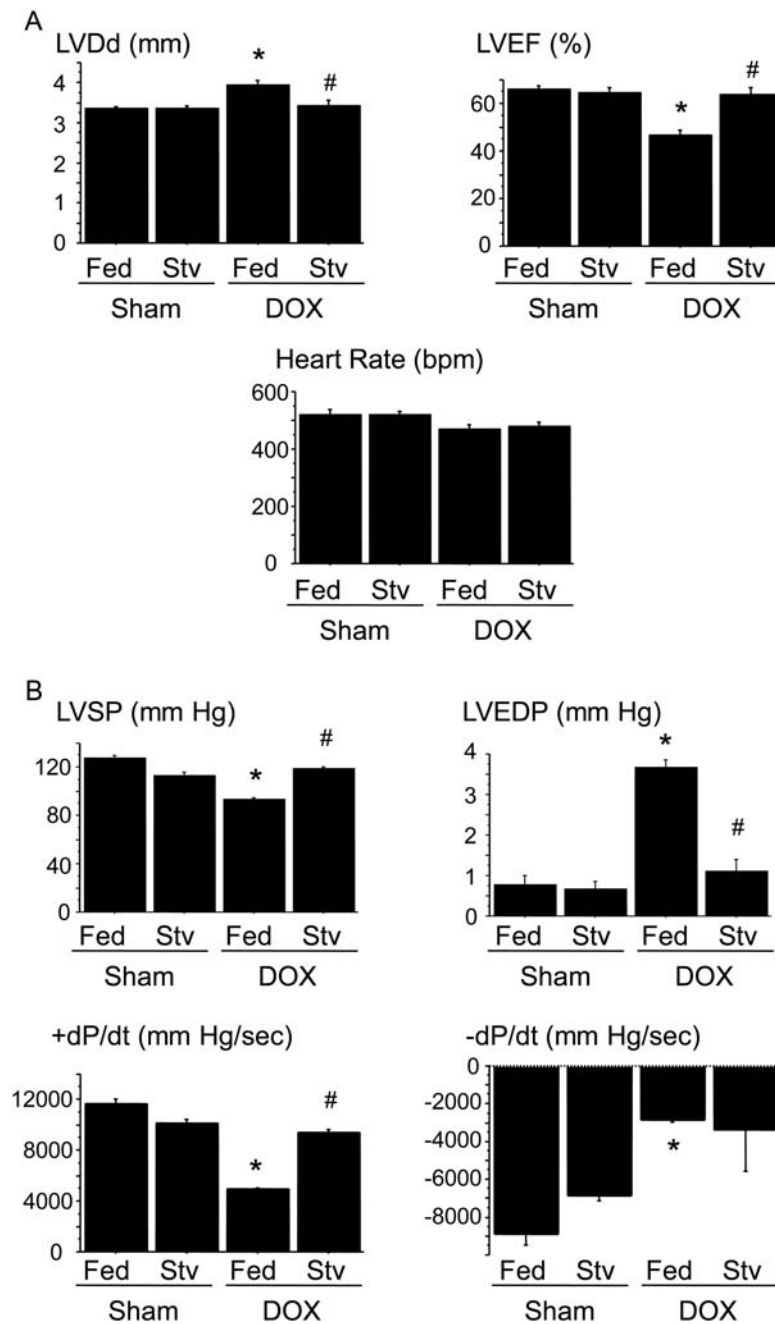


**Figure 1** Effect of starvation (Stv) on left ventricular geometry and function in doxorubicin (DOX) cardiotoxicity evaluated using echocardiography and cardiac catheterization.  $n = 8$  per group; \* $P < 0.05$  vs. the saline (Sham) group without prior starvation [DOX (-) and Stv (-)]; # $P < 0.05$  vs. the DOX group without prior starvation [DOX (+) and Stv (-)].

DOX without prior starvation (Figure 3A). The increase was more marked than that seen in mice starved for 2 days immediately before killing (2-day-starvation control) and, somewhat unexpectedly, than that in mice starved prior to DOX administration (Figure 3A). Western blotting confirmed that LC3-II expression was most prominent in the DOX group without prior starvation (Figure 3B). The myocardial expression profile of the LC3-binding protein p62 paralleled that of LC3-II (Figure 3B). p62 regulates the formation of protein aggregates and is removed by autophagy during the digestion steps.<sup>32</sup> Thus, the accumulation of p62 in the DOX-treated hearts

could be indicative of an inability to complete autophagy. The expression level of cathepsin D, a lysosomal protein, was most prominent in the DOX-treated hearts without prior starvation (Figure 3B).

We next measured myocardial ATP content. As shown in Figure 4A, myocardial ATP content was markedly reduced in mice treated with DOX without prior starvation. Notably, however, ATP levels were nearly fully restored by starvation prior to DOX administration. It was somewhat surprising that in the DOX-treated hearts the ATP levels were reduced in cells overexpressing LC3-II, because one of the functions of autophagy is to supply ATP through recycling. We

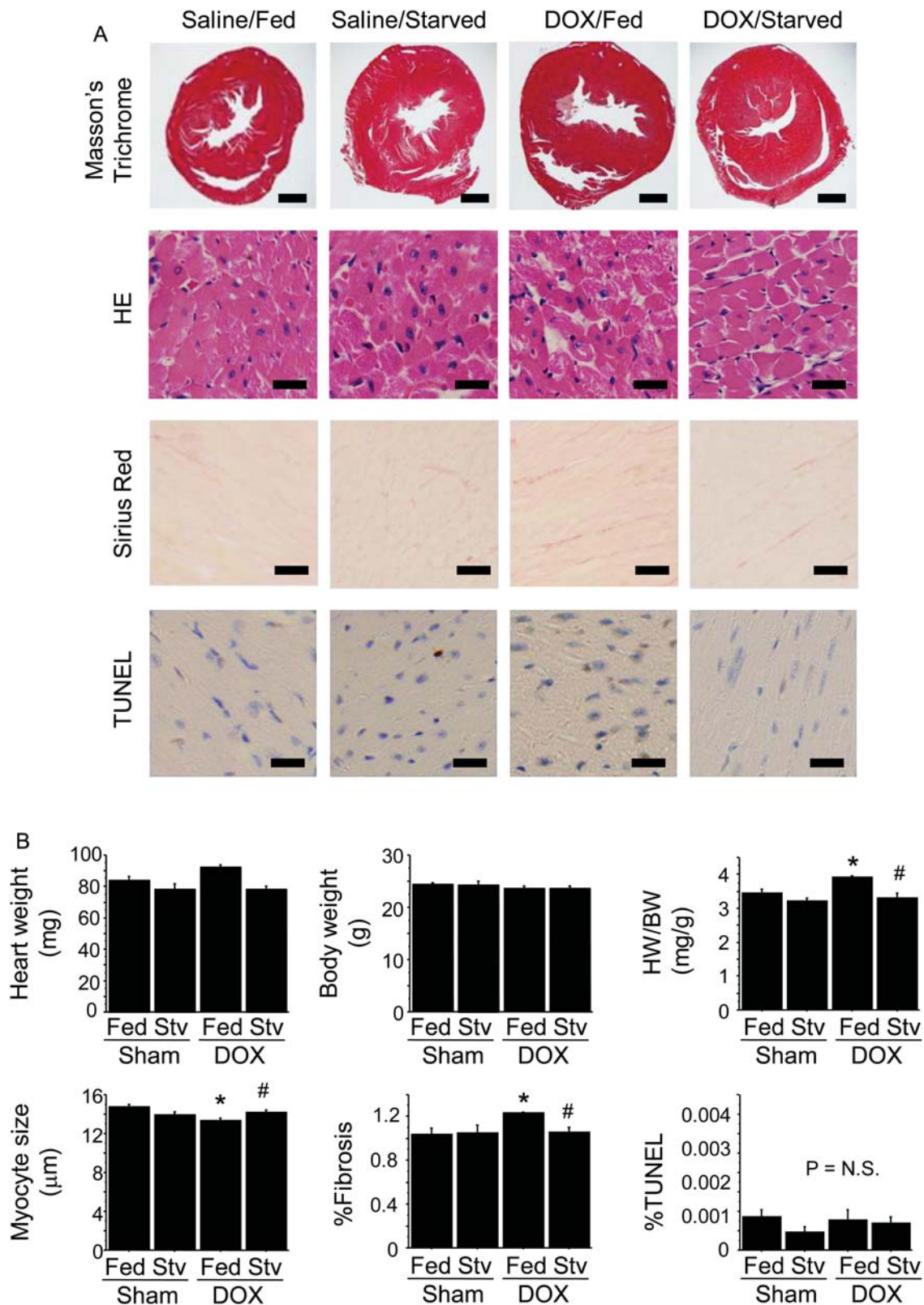


**Figure 2** Effect of starvation on cardiac histology in DOX cardiotoxicity. (A) Photomicrographs of histological [Masson's trichrome, haematoxylin and eosin (HE), and sirius red staining] and TUNEL preparations of heart specimens from the indicated groups. Scale bars represent 20 μm. (B) Graphs showing morphometric data.  $n = 5$  per group; \* $P < 0.05$  vs. the DOX (-) and Stv (-) group; # $P < 0.05$  vs. the DOX (+) and Stv (-) group.

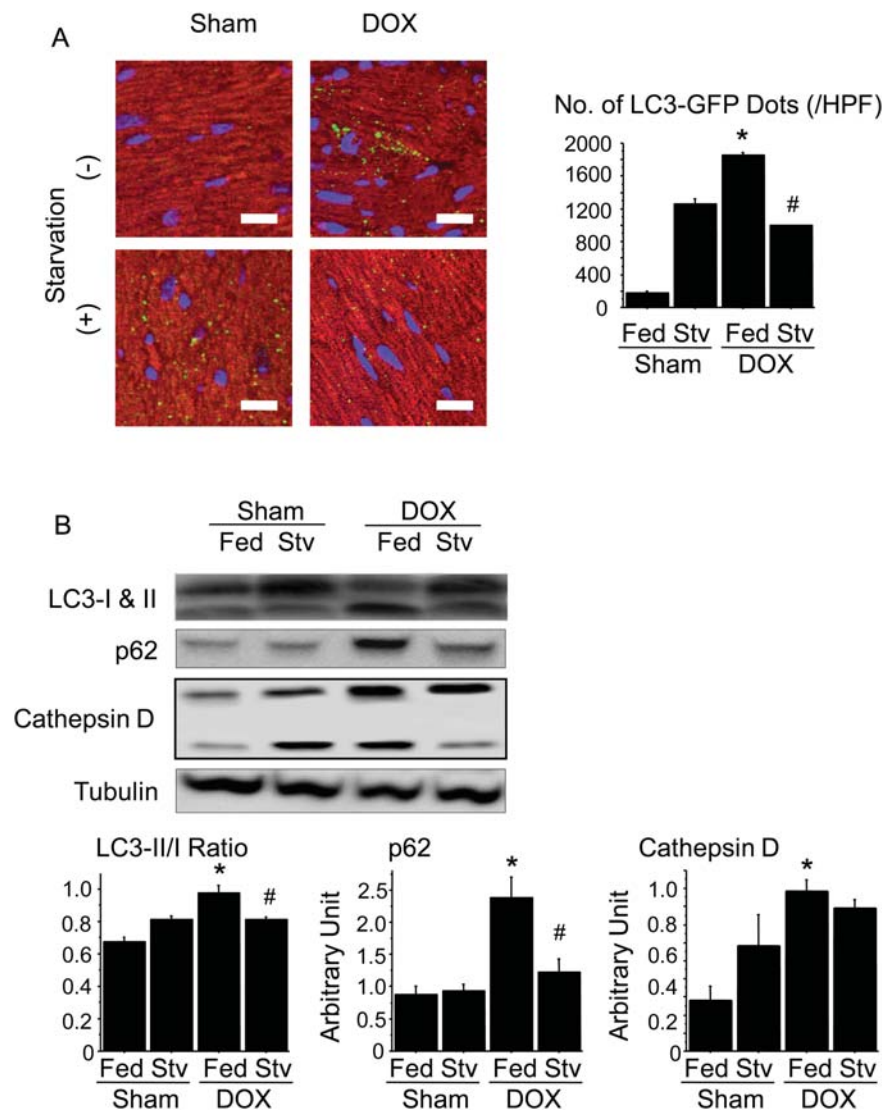


**Figure 3** Effect of starvation on autophagy in DOX cardiotoxicity. (A) Immunohistochemical detection of myocardial LC3-GFP (green). Cardiomyocytes are stained red with rhodamine-phalloidine, and the nuclei are stained blue with Hoechst 33342. The graph shows the levels of LC3-GFP determined from the density (dots per unit area cardiac tissue) of the LC3-GFP puncta.  $n = 8$  per group. Scale bars represent  $20 \mu\text{m}$ . (B) Western blots of myocardial LC3, p62, and cathepsin D. Graphs show the relative myocardial levels of LC3 (left), p62 (middle), and cathepsin D (right) determined from the densitometry.  $n = 5$  per group. \* $P < 0.05$  vs. the DOX (-) and Stv (-) group; # $P < 0.05$  vs. the DOX (+) and Stv (-) group.

therefore used electron microscopy to determine whether, in fact, autophagosomes were being formed in the DOX-treated hearts. We found that typical autophagosomes, including autolysosomes, were rare in DOX-treated hearts (Figure 5). Instead, there were many homogeneously electron-dense vesicles that were previously reported to be lysosomes.<sup>11</sup> Such an ultrastructure, i.e. abundant lysosomes, could be supported by the finding of western blotting for cathepsin D as shown above. However, the prevalence of typical autophagosomes was increased when DOX treatment was preceded by starvation. These findings suggest that the autophagic process has indeed begun to be activated in the DOX-treated heart, but its process is disrupted at a relatively early stage, i.e. before formation of autophagolysosomes, and starvation restores the process.

### 3.4 Autophagic flux in acute DOX cardiotoxicity

To examine whether the observed increase in LC3 expression was due to increased autophagosome formation or impaired autophagosome degradation, we measured autophagic flux *in vivo* after administration of DOX (see Supplementary material online, Figure S1B for the protocol). An increase in the number of LC3 dots was evident under a light microscope in DOX-treated animals. However, treatment with chloroquine produced no further increase in LC3 dots (Figure 6A). Consistent with that finding, western blot analysis showed no increase in chloroquine-induced LC3 activity, evaluated based on the LC3-III/LC3-I ratio in the same experimental setting (Figure 6B).

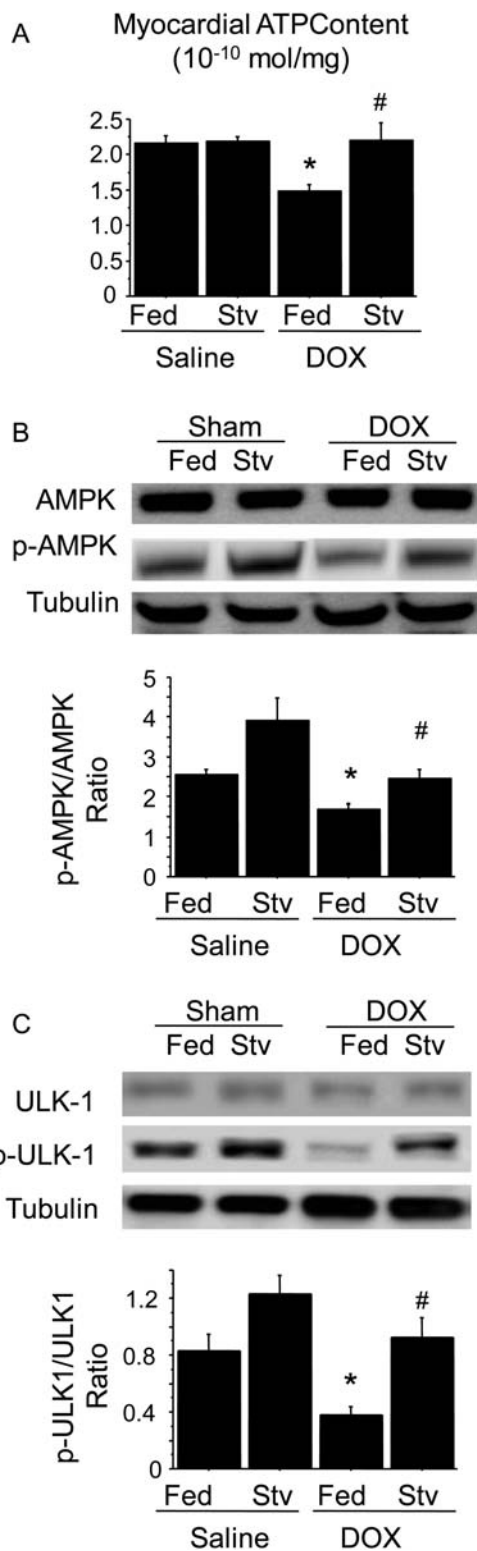


**Figure 4** Energy status in DOX cardiotoxicity. (A) Effect of starvation on myocardial ATP content in DOX cardiotoxicity. (B) Western blots of AMPK and p-AMPK. The graph shows the relative levels of AMPK activation expressed as the p-AMPK/AMPK ratio. (C) Western blots of ULK1 and p-ULK1. The graph shows the relative levels of ULK1 activation expressed as the p-ULK1/ULK1 ratio.  $n = 5$  per group. \* $P < 0.05$  vs. the DOX (-) and Stv (-) group; # $P < 0.05$  vs. the DOX (+) and Stv (-) group.

### 3.5 AMPK and ULK1 activity in the DOX-treated heart

These findings suggest that DOX possibly interferes with the normal flux of autophagy in cardiomyocytes. Thus, we next investigated the underlying molecular mechanisms. AMPK belongs to a conserved family of protein kinases activated by ATP depletion and the resultant AMP accumulation, and is an important regulator of autophagy stimulated by cellular starvation.<sup>33</sup> AMPK activity, assessed based on the myocardial levels of p-AMPK, was significantly increased by starvation, as expected. The activity was significantly reduced by DOX, but the reduction in AMPK activity was significantly mitigated by prior starvation (Figure 4B).

A very recent study reported that direct phosphorylation of the mammalian autophagy-initiating kinase ULK1, a homologue of yeast Atg1, by AMPK is inevitable for induction of autophagy.<sup>34</sup> ULK1 activity, assessed based on the myocardial levels of phosphorylated (Ser317) ULK1, was significantly increased by starvation, as expected. The activity of ULK1 was significantly reduced by DOX, and this reduction was significantly mitigated by prior starvation (Figure 4C).

### 3.6 In vitro studies

We performed experiments using isolated neonatal murine cardiomyocytes to test whether the *in vivo* results are reproducible. First, the cardiomyocytes were exposed to DOX with or without prior culture in glucose-depleted medium. Second, autophagic flux was assayed in the cultured cardiomyocytes. In both of these *in vitro* experiments, the *in vivo* results were completely reproducible, as shown in the Supplementary material online, Figure S3. LC3 expression was most intense, suggesting accelerated autophagy, but autophagic flux was impaired by the treatment with DOX, and the flux was restored by the pre-treatment with glucose depletion (see Supplementary material online, Figure S3A). Although an increase in the number of LC3-GFP dots was evident in DOX-treated cardiomyocytes, treatment with chloroquine produced no further increase in LC3-GFP dots (see Supplementary material online, Figure S3B).

## 4. Discussion

### 4.1 Pathogenic role of autophagy in DOX cardiotoxicity

An increase in autophagic findings was previously reported in a rat model of acute DOX cardiotoxicity.<sup>27</sup> In that model, Beclin-1, a protein known to be involved in autophagosome formation, was up-regulated, and treatment with 3-methyladenine, a class III phosphatidylinositol 3-kinase blocker and autophagy inhibitor,<sup>35</sup> suppressed the upregulation of Beclin-1 and improved cardiac function, suggesting that autophagy exerts a detrimental effect in acute DOX cardiotoxicity. However, the dynamics of cardiac autophagy could not be realized in that study, which lacked analysis of autophagic flux.<sup>27</sup> In addition, 3-methyladenine was recently found to promote autophagy when administered in nutrient-rich conditions for a prolonged period, though it remains capable of inhibiting starvation-induced autophagy.<sup>36</sup> This casts doubt on the validity of using 3-methyladenine to inhibit autophagy *in vivo*. Our present study revealed that in acute DOX cardiotoxicity, autophagic function is impaired, resulting in the accumulation of LC3-II and p62. That accumulation makes it appear, at first glance, that autophagic activity is

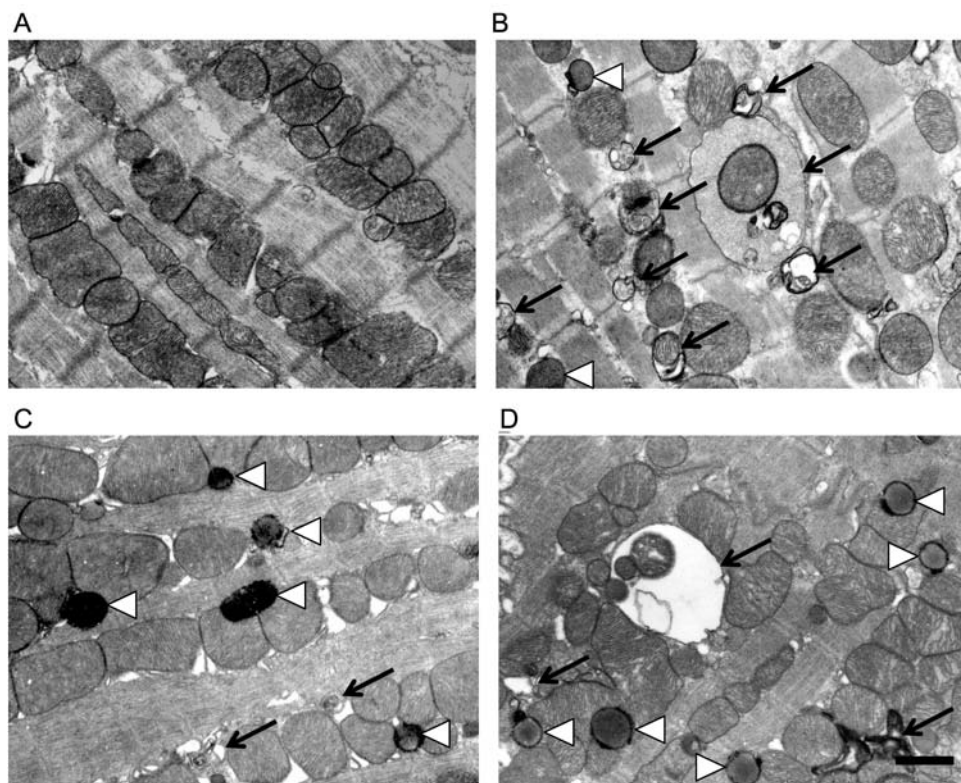


**Figure 5** Autophagic ultrastructure in DOX cardiotoxicity. Electron micrographs of cardiomyocytes from a control mouse (A), a mouse starved for 48 h (B), a mouse treated with DOX (C), and a mouse treated with DOX after undergoing starvation (D). In the DOX-treated hearts, typical autophagosomes were rare, which was in clear contrast to the large numbers seen in the starved control mice (arrows). Instead, DOX-treated hearts exhibited many homogeneously electron-dense vesicles (open arrowheads) that we previously reported to be lysosomes. The prevalence of typical autophagosomes was increased in the DOX-treated hearts when starvation preceded the DOX administration.  $n = 3$  per group. Scale bars represent 1  $\mu\text{m}$ .

increased, but autophagosomes were not abundant at the ultrastructural level, and the energy recycling process is inhibited in DOX-treated hearts. Prior starvation, which induces massive autophagy, appears to restore myocardial ATP levels and improve cardiac function.

Although we linked cardioprotection against DOX cardiotoxicity to autophagy in the present study, the observation of such a cardioprotection by caloric restriction is not new; Mitra *et al.* previously showed that dietary restriction confers resiliency against DOX cardiotoxicity in rats.<sup>37</sup> They suggested the mechanisms to be decreasing oxidative stress, enhancing ATP production, and inducing the JAK/STAT3 pathway. Along with those mechanisms proposed earlier, the present findings appear to provide an additional pathophysiological basis for the benefits of caloric restriction.

Previous findings suggest that apoptosis among cardiomyocytes is increased to be a leading cause of cardiac dysfunction in DOX-induced cardiomyopathy,<sup>38</sup> although this hypothesis is still controversial because of the lack of evidence of apoptotic morphology in those cardiomyocytes.<sup>39–41</sup> Seeking evidence of DOX-induced apoptosis, we conducted a series of TUNEL assays and electron microscopic examinations, but we detected no effect of DOX or starvation on the incidence of apoptosis. Our findings thus suggest that cardiomyocyte apoptosis is not important for disease progression in the present model. The survival rate of the present model was 100% in each

group. These findings suggest that the DOX insult in our model may be too weak to induce death in cardiac cells, compared with the previous studies.

## 4.2 Possible mechanisms for impaired autophagy by DOX treatment

We then tried to elucidate how DOX may possibly interfere with the normal flux of autophagy in cardiomyocytes. We confirmed inactivation of AMPK in DOX cardiotoxicity, which was restored by prior starvation. AMPK is an evolutionarily conserved cellular energy manager that controls nutrient sensing and energy homeostasis. It has been thought that AMPK triggers autophagy through an indirect mechanism, inhibiting mTOR complex 1 activity by phosphorylating tuberous sclerosis type 2 and Raptor.<sup>33,42</sup> Recent studies, however, indicate a more direct mechanism, whereby AMPK regulates autophagy through phosphorylation of ULK1.<sup>43,44</sup> The ULK1 (mammalian homologue of yeast Atg1) kinase complex plays a central role in induction of autophagy. In the present study, we observed a reduced phosphorylation level of ULK1 in DOX cardiotoxicity, which should have resulted in failure to induce autophagy, i.e. the earliest step of autophagosome formation. In addition, prior starvation is suggested to play a role in restoration of this pathway. These findings suggest that AMPK inactivation and the subsequent ULK1 inactivation provide



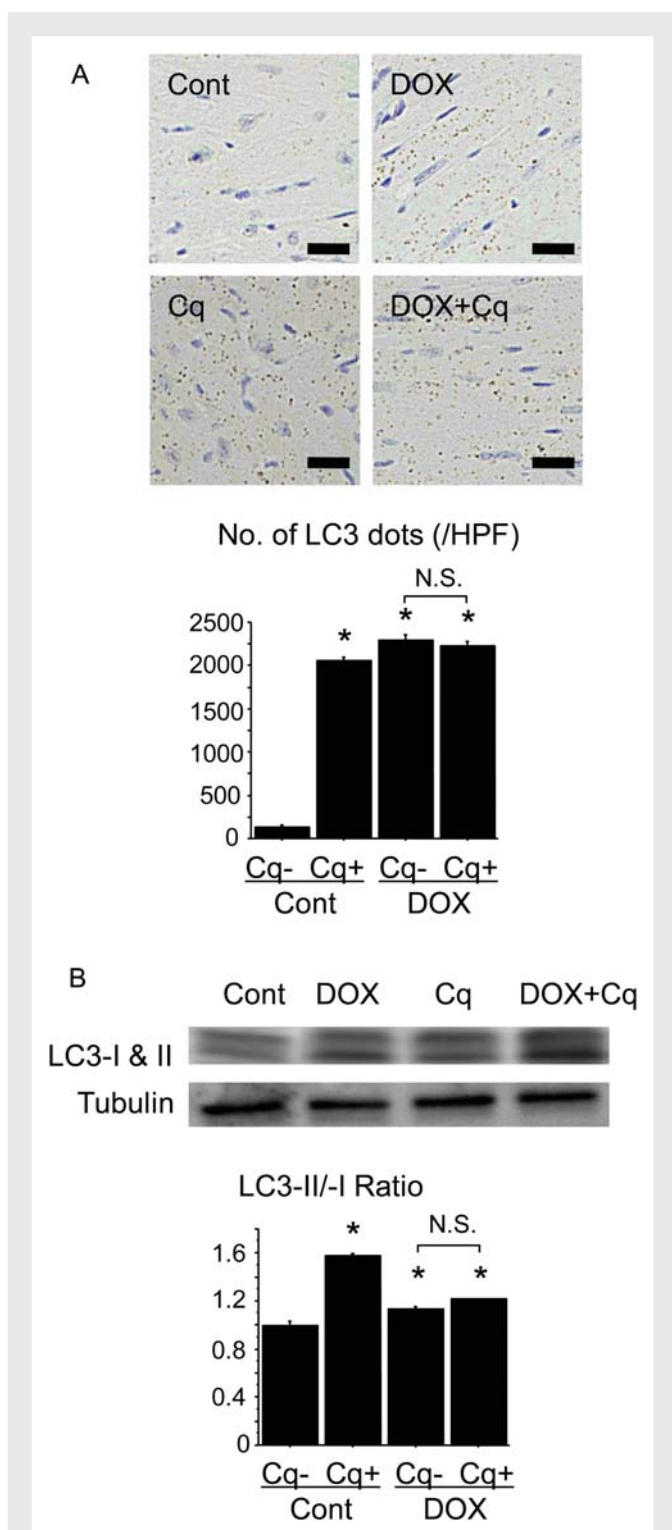


**Figure 6** *In vivo* autophagic flux assay. See Supplementary material online, Figure S1B for the experimental protocol. (A) Immunohistochemical detection of myocardial LC3 (brown dots). The graph shows the levels of LC3 determined from the density (dots per cardiac tissue area) of the LC3 puncta. Scale bars represent 20  $\mu$ m. (B) Western blots of myocardial LC3. The graph shows the relative levels of LC3 determined by densitometry.  $n = 5$  per group. \* $P < 0.05$  vs. the DOX (–) and Stv (–) group; # $P < 0.05$  vs. the DOX (+) and Stv (–) group. Cont, control; DOX, doxorubicin; Cq, chloroquine; DOX+Cq, doxorubicin plus chloroquine.

one possible molecular mechanism for impaired autophagic flux in DOX cardiotoxicity (see Supplementary material online, Figure S4). To confirm this hypothesis, however, further experiments are warranted, using pharmacological or genetic approaches.

The mechanisms proposed by the present study for DOX-induced impairment of autophagy may be somewhat confusing; the data with LC3, p62, and autophagic flux assay with chloroquine support the finding that DOX increases autophagosome formation but impairs its degradation, whereas the electron microscopic findings and AMPK-ULK1 data support the finding that DOX impairs autophagosome formation. Although LC3-II is indeed a well-established marker for autophagosome formation, activation of many other autophagy-related proteins are required for the formation;<sup>1,2</sup> otherwise, the formation would be incomplete. It is easily surmised that such incomplete autophagosomes without a visible membrane could affect the subsequent step, i.e. those autophagosomes might not be able to proceed to the next degradation step of autophagy, speculatively, for example, by an inability to fuse with lysosomes, resulting in accumulation of the intact components other than ULK1, such as LC3, p62, and lysosomes, and delay of the flux. Thus, we suppose that the formation of autophagosomes is the major impaired step of autophagy by DOX. However, it is necessary to investigate in future whether or not the degradation step is also impaired.

Compared with the molecular pathways for autophagosome formation, those for lysosomal activation are less well known. During starvation, however, lysosomes appear in the cardiomyocytes more rapidly than the formation of typical autophagosomes.<sup>11</sup> The present study showed a dissociation between the formation of autophagosomes and the appearance of lysosomes in cardiomyocytes of the DOX-treated heart; there were rare autophagosomes and abundant lysosomes. These findings suggest that autophagosomes and lysosomes are differently regulated in their formation process, although the initiation of their formation is triggered by the common stimulus.

### 4.3 Clinical implication

The dose-dependent cardiotoxicity of DOX, leading to irreversible degenerative cardiomyopathy that progresses to congestive heart failure, limits its clinical application. In the present study, we found that starvation for 2 days before DOX treatment significantly mitigated acute DOX cardiotoxicity in mice. The prior starvation significantly restored autophagic function, including myocardial ATP preservation, which was otherwise disrupted by DOX. A recent *in vitro* study using cultured cardiomyocytes reported that DOX-induced cardiomyocyte death was prevented to a significant degree by the glucose analogue 2-deoxy-D-glucose, which mimics caloric restriction in several animal models.<sup>45</sup> The underlying mechanisms included preservation of ATP content in cultured cardiomyocytes, which supports our *in vivo* findings. We therefore propose that fasting or caloric restriction could be a useful strategy for preventing or mitigating DOX cardiotoxicity. We suggest that a strict protocol of fasting be carefully established for cancer patients treated with DOX through extensive studies examining the precise mechanisms, effectiveness, and safety of this therapy.

### 4.4 Conclusion

A period of starvation prior to DOX administration mitigates the acute cardiotoxicity of this drug. The underlying mechanism may be, at least in part, restoration and augmentation of myocardial

autophagy, the flux of which is impaired by DOX, probably through inactivation of AMPK and ULK1. These findings imply that fasting or caloric restriction could be a possible strategy for preventing or mitigating DOX cardiotoxicity.

## Supplementary material

Supplementary material is available at *Cardiovascular Research* online.

## Acknowledgements

We thank the staff of Kyoto Women's University (Yumi Azuma, Erina Ogawa, Chika Kuzumoto, Yoriko Kubo, Yuka Saito, and Sawako Takeuchi) for technical assistance.

**Conflict of interest:** none declared.

## Funding

This study was supported in part by Grants-in-Aid for scientific research from The Ministry of Education, Science, and Culture of Japan, and Research Grants from Gifu University.

## References

- Nakatogawa H, Suzuki K, Kamada Y, Ohsumi Y. Dynamics and diversity in autophagy mechanisms: lessons from yeast. *Nat Rev Mol Cell Biol* 2009;**10**:458–467.
- Mizushima N, Yoshimori T, Ohsumi Y. The role of Atg proteins in autophagosome formation. *Annu Rev Cell Dev Biol* 2011;**27**:107–132.
- Shintani T, Klionsky DJ. Autophagy in health and disease: a double-edged sword. *Science* 2004;**306**:990–995.
- Rubinsztein DC, DiFiglia M, Heintz N, Nixon RA, Ravikumar B et al. Autophagy and its possible roles in nervous system diseases, damage and repair. *Autophagy* 2005;**1**:11–22.
- Schmid D, Münz C. Innate and adaptive immunity through autophagy. *Immunity* 2007;**27**:11–21.
- Tsujimoto Y, Shimizu S. Another way to die: autophagic programmed cell death. *Cell Death Differ* 2005;**12**(Suppl 2):1528–1534.
- Yan L, Vatner DE, Kim SJ, Ge H, Masarekar M, Massover WH et al. Autophagy in chronically ischemic myocardium. *Proc Natl Acad Sci USA* 2005;**102**:13807–13812.
- Takemura G, Miyata S, Kawase Y, Okada H, Maruyama R, Fujiwara H. Autophagic degeneration and death of cardiomyocytes in heart failure. *Autophagy* 2006;**2**:212–214.
- Hein S, Arnon E, Kostin S, Schönburg M, Elsässer A, Polyakova V et al. Progression from compensated hypertrophy to failure in the pressure-overloaded human heart: structural deterioration and compensatory mechanisms. *Circulation* 2003;**107**:984–991.
- Kanamori H, Takemura G, Goto K, Maruyama R, Tsujimoto A, Ogino A et al. The role of autophagy emerging in postinfarction cardiac remodeling. *Cardiovasc Res* 2011;**91**:330–339.
- Kanamori H, Takemura G, Maruyama R, Goto K, Tsujimoto A, Ogino A et al. Functional significance and morphological characterization of starvation-induced autophagy in the adult heart. *Am J Pathol* 2009;**174**:1705–1714.
- Nakai A, Yamaguchi O, Takeda T, Higuchi Y, Hikoso S, Taniike M et al. The role of autophagy in cardiomyocytes in the basal state and in response to hemodynamic stress. *Nat Med* 2007;**13**:619–624.
- Matsui Y, Takagi H, Qu X, Abdellatif M, Sakoda H, Asano T et al. Distinct roles of autophagy in the heart during ischemia and reperfusion: roles of AMP-activated protein kinase and Beclin 1 in mediating autophagy. *Circ Res* 2007;**100**:914–922.
- Kanamori H, Takemura G, Goto K, Maruyama R, Ono K, Nagao K et al. Autophagy limits acute myocardial infarction induced by permanent coronary artery occlusion. *Am J Physiol Heart Circ Physiol* 2011;**300**:H2261–H2271.
- Clarke PG. Developmental cell death: morphological diversity and multiple mechanisms. *Anat Embryol* 1990;**181**:195–213.
- De Meyer GR, Martinet W. Autophagy in the cardiovascular system. *Biochim Biophys Acta* 2009;**1793**:1485–1495.
- Gustafsson AB, Gottlieb RA. Heart mitochondria: gates of life and death. *Cardiovasc Res* 2008;**77**:334–343.
- Matsui Y, Kyoi S, Takagi H, Hsu CP, Hariharan N, Ago T et al. Molecular mechanisms and physiological significance of autophagy during myocardial ischemia and reperfusion. *Autophagy* 2008;**4**:409–415.
- Rothermel BA, Hill JA. Autophagy in load-induced heart disease. *Circ Res* 2008;**103**:1363–1369.
- Shimomura H, Terasaki F, Hayashi T, Kitaura Y, Isomura T, Suma H. Autophagic degeneration as a possible mechanism of myocardial cell death in dilated cardiomyopathy. *Jpn Circ J* 2001;**65**:965–968.
- Terman A, Brunk UT. Autophagy in cardiac myocyte homeostasis, aging, and pathology. *Cardiovasc Res* 2005;**68**:355–365.
- Bristow MR, Billingham ME, Mason JW, Daniels JR. Clinical spectrum of anthracycline antibiotic cardiotoxicity. *Cancer Treat Rep* 1978;**62**:873–879.
- Singal PK, Iliskovic N. Doxorubicin-induced cardiomyopathy. *N Engl J Med* 1998;**339**:900–905.
- Takemura G, Fujiwara H. Doxorubicin-induced cardiomyopathy from the cardiotoxic mechanisms to management. *Prog Cardiovasc Dis* 2007;**49**:330–352.
- Zhou S, Starkov A, Froberg MK, Leino RL, Wallace KB. Cumulative and irreversible cardiac mitochondrial dysfunction induced by doxorubicin. *Cancer Res* 2001;**61**:771–777.
- Zhu W, Soonpaa MH, Chen H, Shen W, Payne RM, Liechty EA et al. Acute doxorubicin cardiotoxicity is associated with p53-induced inhibition of the mammalian target of rapamycin pathway. *Circulation* 2009;**119**:99–106.
- Lu L, Wu W, Yan J, Li X, Yu H, Yu X. Adriamycin-induced autophagic cardiomyocyte death plays a pathogenic role in a rat model of heart failure. *Int J Cardiol* 2009;**134**:82–90.
- Mizushima N, Yamamoto A, Matsui M, Yoshimori T, Ohsumi Y. In vivo analysis of autophagy in response to nutrient starvation using transgenic mice expressing a fluorescent autophagosome marker. *Mol Biol Cell* 2004;**15**:1101–1111.
- Iwai-Kanai E, Yuan H, Huang C, Sayen MR, Perry-Garza CN, Kim L et al. A method to measure cardiac autophagic flux in vivo. *Autophagy* 2008;**4**:322–329.
- Buss SJ, Muenz S, Riffel JH, Malekar P, Hagenmueller M, Weiss CS et al. Beneficial effects of Mammalian target of rapamycin inhibition on left ventricular remodeling after myocardial infarction. *J Am Coll Cardiol* 2009;**54**:2435–2446.
- Wang L, Feng ZP, Kondo CS, Sheldon RS, Duff HJ. Developmental changes in the delayed rectifier K<sup>+</sup> channels in mouse heart. *Circ Res* 1996;**79**:79–85.
- Komatsu M, Waguri S, Koike M, Sou YS, Ueno T, Hara T et al. Homeostatic levels of p62 control cytoplasmic inclusion body formation in autophagy-deficient mice. *Cell* 2007;**131**:1149–1163.
- Inoki K, Zhu T, Guan KL. TSC2 mediates cellular energy response to control cell growth and survival. *Cell* 2003;**115**:577–590.
- Lee JW, Park S, Takahashi Y, Wang HG. The association of AMPK with ULK1 regulates autophagy. *PLoS One* 2010;**5**:e15394.
- Seglen PO, Gordon PB. 3-Methyladenine: specific inhibitor of autophagic/lysosomal protein degradation in isolated rat hepatocytes. *Proc Natl Acad Sci USA* 1982;**79**:1889–1892.
- Wu YT, Tan HL, Shui G, Bauvy C, Huang Q, Wenk MR et al. Dual role of 3-methyladenine in modulation of autophagy via different temporal patterns of inhibition on class I and III phosphoinositide 3-kinase. *J Biol Chem* 2010;**285**:10850–10861.
- Mitra MS, Donthamsetty S, White B, Latendresse JR, Mehendale HM. Mechanism of protection of moderately diet restricted rats against doxorubicin-induced acute cardiotoxicity. *Toxicol Appl Pharmacol* 2007;**225**:90–101.
- Kalyanaraman B, Joseph J, Kalivendi S, Wang S, Konorev E, Kotamraju S. Doxorubicin-induced apoptosis: implications in cardiotoxicity. *Mol Cell Biochem* 2002;**234–235**:119–124.
- Rosenoff SH, Olson HM, Young DM, Bostick F, Young RC. Adriamycin-induced cardiac damage in the mouse: a small-animal model of cardiotoxicity. *J Natl Cancer Inst* 1975;**55**:191–194.
- Zhang J, Clark JR Jr, Herman EH, Ferrans V. Doxorubicin-induced apoptosis in spontaneously hypertensive rats: differential effects in heart, kidney and intestine, and inhibition by ICRF-187. *J Mol Cell Cardiol* 1996;**28**:1931–1943.
- Li L, Takemura G, Li Y, Miyata S, Esaki M, Okada H et al. Preventive effect of erythropoietin on cardiac dysfunction in doxorubicin-induced cardiomyopathy. *Circulation* 2006;**113**:535–543.
- Gwinn DM, Shackelford DB, Egan DF, Mihaylova MM, Mery A, Vasquez DS et al. AMPK phosphorylation of raptor mediates a metabolic checkpoint. *Mol Cell* 2008;**30**:214–226.
- Egan DF, Shackelford DB, Mihaylova MM, Gelino S, Kohnz RA, Mair W et al. Phosphorylation of ULK1 (hATG1) by AMP-activated protein kinase connects energy sensing to mitophagy. *Science* 2011;**331**:456–461.
- Kim J, Kundu M, Viollet B, Guan KL. AMPK and mTOR regulate autophagy through direct phosphorylation of Ulk1. *Nat Cell Biol* 2011;**13**:132–141.
- Chen K, Xu X, Kobayashi S, Timm D, Jepperson T, Liang Q. Caloric restriction mimetic 2-deoxyglucose antagonizes doxorubicin-induced cardiomyocyte death by multiple mechanisms. *J Biol Chem* 2011;**286**:21993–22006.